International Immunopharmacology 76 (2019) 105791

Contents lists available at ScienceDirect

International Immunopharmacology

journal homepage: www.elsevier.com/locate/intimp

Accumulation of cytosolic dsDNA contributes to fibroblast-like synoviocytes-mediated rheumatoid arthritis synovial inflammation☆

Jingnan Wang[a,1], Ruiru Li[a,1], Haobo Lin[b,1], Qian Qiu[a], Minxi Lao[a], Shan Zeng[a], Cuicui Wang[a], Siqi Xu[a], Yaoyao Zou[a], Maohua Shi[a], Liuqin Liang[a], Hanshi Xu[a], Youjun Xiao[a,*]

[a] Department of Rheumatology and Clinical Immunology, The First Affiliated Hospital, Sun Yat-sen University, Guangzhou, Guangdong, China
[b] Department of Rheumatology, Guangdong Provincial People's Hospital, Guangdong Academy of Medical Sciences, Guangzhou, Guangdong, China

ARTICLE INFO

Keywords:
Cytosolic dsDNA
Inflammation
cGAS
FLS
Rheumatoid arthritis

ABSTRACT

The accumulation of cytosolic dsDNA plays important roles in the regulation of cellular processes. However, whether cytosolic dsDNA is involved in the pathogenesis of rheumatoid arthritis (RA) is not clear. Therefore, the present study investigated the roles of cytosolic dsDNA in the modulation of inflammatory responses of fibroblast-like synoviocytes (FLS) in patients with RA. FLS were obtained from active RA patients. dsDNA accumulation in the cytosol was detected by immunofluorescence staining and the Qubit® dsDNA HS Assay. Immunohistochemistry was employed to detect the dsDNA and cGMP-AMP synthase (cGAS) expression in the synovium. Short hairpin RNA (shRNA) was used to knockdown the expression of cGAS and stimulator of interferon genes (STING). Protein expression was detected by Western blotting and immunofluorescence staining. We observed increased cytosolic dsDNA and cGAS expression in FLS and synovium from RA patients. dsDNA and cGAS expression correlated with the severity of rheumatoid synovitis. Transfection of dsDNA into the cytosol of RA FLS promoted pro-inflammatory cytokines production. DNaseII overexpression downregulated cytosolic dsDNA expression and inhibited dsDNA-induced cytokines secretion. We also found that dsDNA and TNF-α enhanced cGAS and STING expression, and dsDNA-induced cytokine secretion was reduced by cGAS or STING knockdown. Furthermore, we determined that the dsDNA-induced phosphorylation of IRF3 and NF-κBp65 was decreased by DNaseII overexpression or cGAS/STING knockdown. Overall, our findings show that increased cytosolic dsDNA level promoted inflammatory responses via the cGAS/STING pathway in RA FLS, which suggests that cytosolic dsDNA accumulation is an important contributor to FLS-mediated rheumatoid synovial inflammation.

1. Introduction

The cytosol is devoid of DNA under normal circumstances, but DNA enters the cytoplasm under certain circumstances of stress or damage. DNA accumulation in the cytosol results in activation of the innate immune response and a subsequent pro-inflammatory cytokines production, which can be both beneficial and detrimental. Cytosolic DNA sensing initiates antiviral immunity and autoimmunity. Cyclic-GMP-AMP synthase (cGAS), DDX41, IFI16, LRRFIP1, Ku70 and DAI are receptors involved in DNA recognition. cGAS appears indispensable for the IFN response to cytosolic DNA. cGAS binds to dsDNA, which results in cyclic-GMP-AMP production and STING activation to encode type I IFN and pro-inflammatory cytokines via activation of transcription factors IRF3 and the NF-κB signaling pathway [1,2].

Rheumatoid arthritis (RA) is a common autoimmune disease that is characterized by chronic synovial inflammation and progressive joint destruction. Fibroblast-like synoviocytes (FLS) in the synovial intimal lining play a critical role in the initiation and perpetuation of joint

Abbreviations: cGAS, cyclic-GMP-AMP synthase; STING, stimulator of interferon genes; FLS, fibroblast-like synoviocytes; TNF-α, tumor necrosis factor-α; RA, rheumatoid arthritis; MMP, matrix metalloproteinases; HC, healthy control; OA, osteoarthritis; CTR, control

☆ This work was supported by grants from National Natural Science Foundation of China (Grant numbers U1401222, 81671591, 81373182, 81501389, 81601437, 81701611, 81601403 and 81871275), Natural Science Foundation of Guangdong Province (Grant numbers S2013010015363, 2015A030313012), Guangdong Science and Technology Department (Grant numbers 2014A020212144, 2016A020215051).

* Corresponding author at: Department of Rheumatology, The First Affiliated Hospital, Sun Yat-sen University, No. 58 Zhongshan Road 2, Guangzhou, Guangdong 510080, Republic of China.
E-mail address: xiaoyouj@mail2.sysu.edu.cn (Y. Xiao).

[1] Wang J, Li R and Lin H shared first authorship.

https://doi.org/10.1016/j.intimp.2019.105791
Received 3 March 2019; Received in revised form 24 July 2019; Accepted 25 July 2019
Available online 28 August 2019

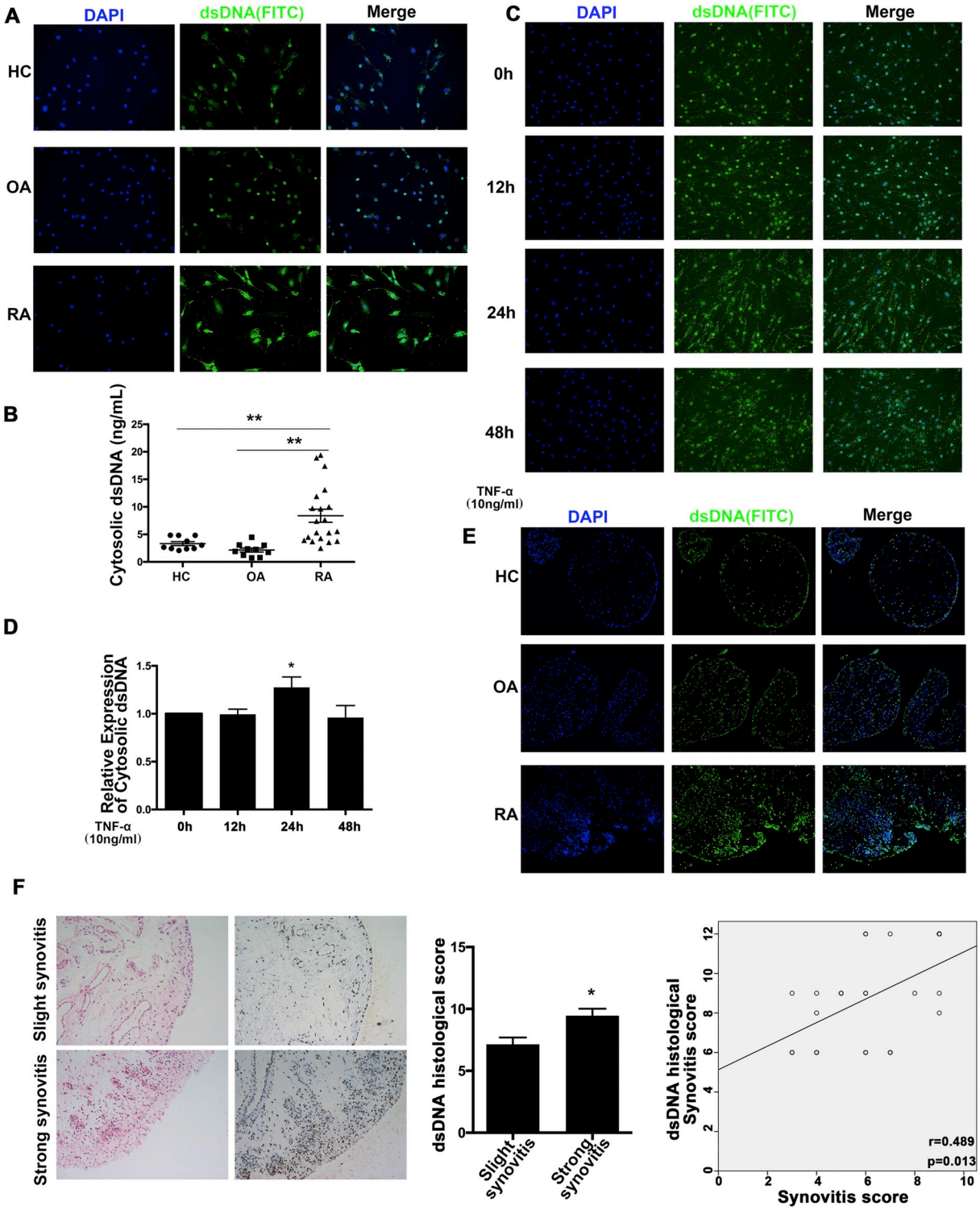

Fig. 1. Increased expression of dsDNA in synovial tissue and FLS from patients with RA. (A) dsDNA expression in FLS was detected using immunofluorescent staining. Representative images of dsDNA (green) and nuclei (blue) in FLS from HC (n = 4) and patients with OA (n = 6) and RA (n = 8). Original magnification 200×. (B) Cytosolic dsDNA of FLS was determined using Qubit® dsDNA HS Assay. Graph represents the content of dsDNA in the cytosol of FLS from HC (n = 10) and patients with OA (n = 10) and RA (n = 20). Data are shown as the means ± SEM. $^{**}P < 0.01$, versus HC or OA patients, using one-way ANOVA assay with Bonferroni's post hoc comparison. (C and D) RA-FLS were stimulated with TNF-α (10 ng/ml) for 12, 24 and 48 h. dsDNA expression was detected using immunofluorescent staining and Qubit® dsDNA HS Assay. Representative images of immunofluorescent staining (original magnification 200×) are shown. Graph represents the relative expression of cytosolic dsDNA in the RA FLS with TNF-α stimulation. Data were normalized to the control group (0 h) and are presented as the means ± SEM of 6 independent experiments. $^{*}P < 0.05$, versus 0 h, using one-way ANOVA assay with Bonferroni's post hoc comparison. (E) dsDNA expression in the synovium from HC (n = 4), OA patients (n = 6) and RA patients (n = 8). Representative images of immunofluorescent staining (original magnification 200×) are shown. (F) dsDNA expression and synovitis evaluation were detected using immunohistochemistry and H&E staining, respectively. Graph indicates dsDNA histological scores in slight and strong synovitis. Data are shown as the means ± SEM of 24 independent experiments involving 24 different RA patients. $^{*}P < 0.05$, versus slight synovitis, using Student's t-test. Correlations analyses were analyzed using Spearman's rank order correlation test. (For interpretation of the references to colour in this figure legend, the reader is referred to the web version of this article.)

inflammation and cartilage destruction in RA. RA FLS exhibit increased ability to secrete a series of pro-inflammatory cytokines and mediators and matrix metalloproteinases (MMPs). The importance of pro-inflammatory cytokines in synovial inflammation was determined after the success of biologics RA treatment, which blocks the effects of cytokines, such as TNF-α and IL-6 [3,4]. Control of RA FLS-mediated synovial inflammation may represent an important therapeutic target for RA.

cGAS was overexpressed in RA-FLS compared with OA FLS. Besides, TNF-α stimulation can upregulate cGAS expression in RA FLS [5]. Increasing evidences indicates that cytosolic dsDNA from infections or cellular damage contributes to host defense and the pathogenesis of cancer and autoimmune diseases, such as systemic lupus erythematosus and Aicardi-Goutières syndrome (AGS) [6]. Recent studies demonstrated that the cytosolic dsDNA can activate dendritic cells [7], cancer cells [8], and keratinocytes [9]. However, whether cytosolic dsDNA in RA FLS is associated with the pathogenesis of RA is unknown. The present study measured the accumulation of cytosolic dsDNA in FLS and synovium from RA patients and demonstrated an important role of cytosolic dsDNA in the regulation of inflammatory responses of RA FLS via the cGAS/STING pathway. These novel results suggest that increased cytosolic dsDNA levels is involved in FLS-mediated joint inflammation.

2. Materials and methods

2.1. Materials

dsDNA (ISD, E.coli and HSV) was synthesized commercially with the following: ISD (sequence listed in Table S1) (Sangon, Shanghai, China); *E. coli*: #tlrl-ecdna (InvivoGen, USA); HSV, #tlrl-hsv60n (InvivoGen, USA). Primary antibodies used in the immunoblotting assay were as follows: cGAS, STING, p-p65((Ser536))/p65, p-IRF3(Ser396)/IRF3 (Cell Signaling Technology, USA); dsDNA, DNaseII (Abcam, Cambridge, UK); GAPDH (Sigma, USA). ELISA kits were purchased from R&D Systems (USA). Recombinant human TNF-α was purchased from R&D Systems (Minneapolis, MN, USA).

2.2. Methods

2.2.1. Preparation of human FLS and FLS infection

Synovial tissues were obtained from active RA, OA and trauma patients (20 RA women and 5 RA men, aged 42–63 years; 12 OA women and 2 men, aged 55–68 years; 10 trauma patients, aged 45–65 years), who were undergoing joint replacement or synovectomy. RA was diagnosed according to the 2010 American College of Rheumatology/European League Against Rheumatism (ACR/EULAR) classification criteria [10]. The study was performed according to the recommendations of the Declaration of Helsinki and approved by the Medical Ethical Committee of the First Affiliated Hospital, Sun Yat-sen University, China. All patients gave informed consent to participate in the study. Freshly isolated synovial tissues were cut into small pieces and incubated with collagenase for 2–4 h at 37 °C in a 5% CO_2 incubator to isolate FLS. The FLS were cultured in DMEM/F12 (Gibco, USA) medium containing 10% bovine serum (Biological Industries, Israel), 100 U/ml penicillin, and 100 μg/ml streptomycin at 37 °C in a 5% CO_2 incubator. FLS were routinely trypsinized and passaged at sub-confluence (70%–80%). The 4th to 6th passages of FLS were used in our experiments, when the cells were a homogeneous population (< 1% CD11b positive, < 1% phagocytic, and < 1% FcgRII and FcgRIII receptor positive). For lentiviral transductions, cells were grown to 70% confluence and inoculated with lentivirus in the presence of 10 μg/ml polybrene. The media were removed and replaced with fresh media 8 h after transfection. All transfection media were incubated for 48–72 h to allow for protein expression. The infection efficiency was confirmed post-infection by using GFP expression under fluorescence microscopy and measured using Western blotting for cGAS, STING and DNaseII expression.

2.2.2. Cytoplasmic and nuclear gradient extraction and cytosolic dsDNA detection

We used the NE-PER Nuclear and Cytoplasmic Extraction Reagents (Thermo scientific, USA) to extract the cytoplasmic and nuclear gradient, and experiments were performed according to the manufacturer's instruction. The cytoplasmic gradient was stored for the detection of the cytosolic dsDNA. We used the Qubit® dsDNA HS Assay Kits (Invitrogen, USA) to detect the cytosolic dsDNA, and experiments were performed according to the manufacturer's instructions.

2.2.3. Knockdown and overexpression constructs

Lentivirus-mediated shRNA vectors targeting cGAS and STING were constructed as described previously [11]. Table S2 lists the shRNA sequences. Briefly, gene-specific or scramble shRNA sequences were cloned into pLKO.1 vectors (Addgene, Cambridge, MA, USA). PLKO.1 containing cGAS shRNA, STING shRNA and control shRNA was co-transfected with plasmid pCMV-dR8.2-vprX and pCMV-VSVG in HEK293T cells using Lipofectamine 3000 (Life Technologies, USA) according to the manufacturer's protocol. Lentiviral particles were collected from cell supernatants after 48 and 72 h, purified using a 0.45 μM filter.

The ORF lentiviral expression vector pReceiver-Lv105-A0792 (MDK) for the overexpression of human DNaseII and the corresponding empty vector were purchased from GeneCopoeia.

2.2.4. Realtime-PCR

Total RNA was extracted using TRIzol reagent (Sigma, USA). RNA was then reverse-transcribed by using PrimeScript™ RT Master Mix (Takara, Japan). Quantitative real-time PCR analysis was performed using SYBR Premix Ex Taq (Takara, Japan) according to the manufacturer's instructions. Table S1 shows the primer sequences.

2.2.5. Immunofluorescence

FLS were fixed using 4% paraformaldehyde in phosphate-buffered saline (PBS) for 15 min at room temperature and blocked in blocking buffer/0.1% Triton™ X-100 for 1 h. Cells were incubated overnight with diluted primary antibodies at 4 °C and incubated with fluorochrome-conjugated secondary antibodies (Invitrogen, USA) for 1 h at room temperature. Cells were stained using DAPI (BBI, China) and mounted using Fluoroshield™ histology mounting medium (Sigma, USA). Paraffin sections were deparaffinized in xylene and were rehydrated. We performed the antigen retrieval step in 10 mM sodium citrate buffer. Sections were blocked in blocking buffer and incubated in diluted primary antibodies at 4 °C overnight. The subsequent steps were performed as described above.

2.2.6. Cytokines assay

The levels of cytokines, including IL-1β, TNF-α, MMP-13, CXCL-10, IL-6, IL-8, IFN-α, IFN-β and IFN-γ in the supernatants of RA FLS were detected using ELISA (R&D Systems, USA) according to the manufacturer's instructions.

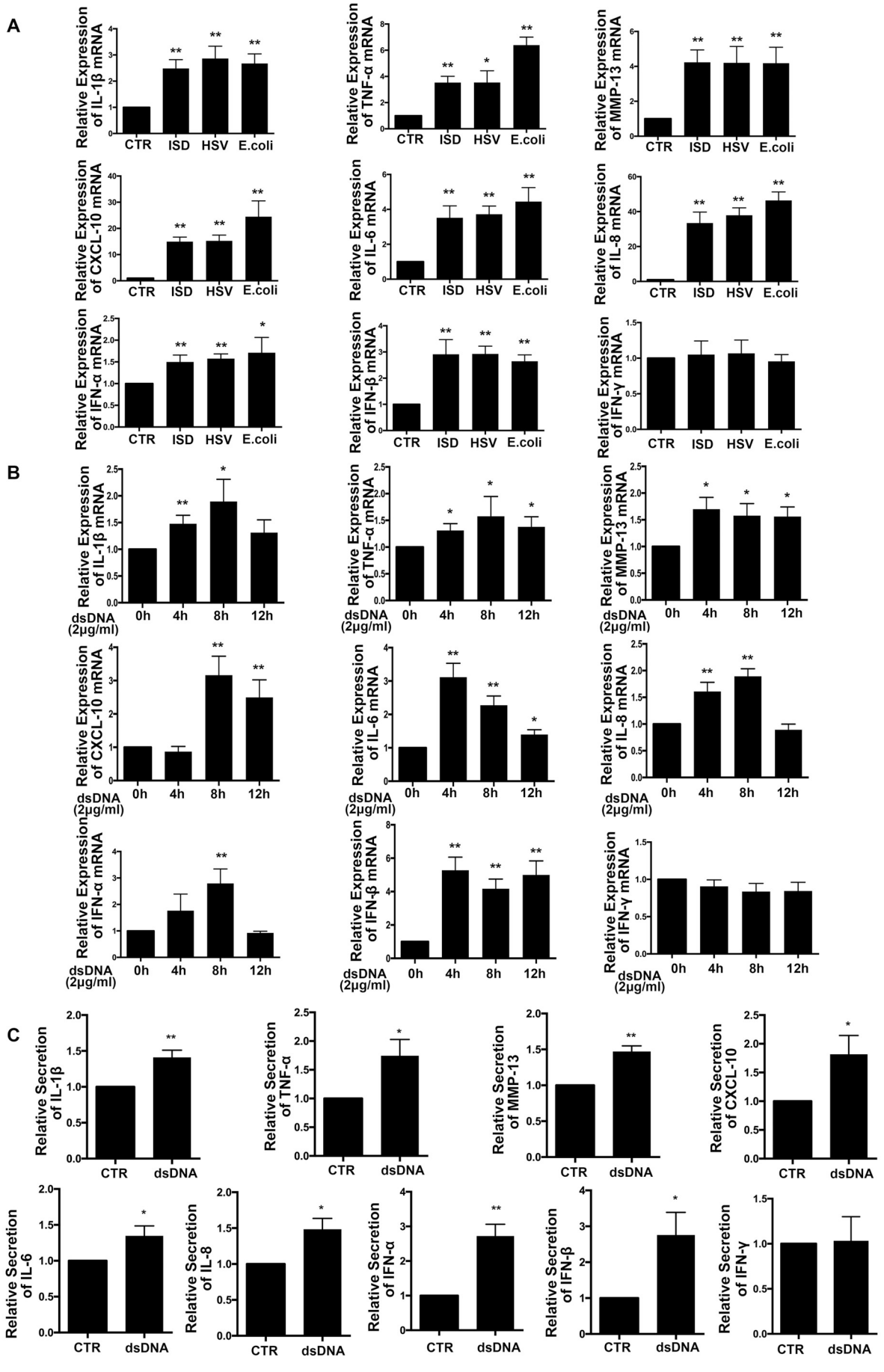

(caption on next page)

Fig. 2. *Effect of cytosolic dsDNA on synovial inflammation.* (A and B) 2 μg/ml dsDNA, including HSV, *E. coli* and ISD dsDNA, was transfected into RA FLS using Lipo3000. Cytokines (IL-1β, TNF-α, MMP-13, CXCL-10, IL-6, IL-8, IFN-α, IFN-β and IFN-γ) mRNA expression was measured using real-time PCR. Graphs indicate the relative mRNA expression. *P < 0.05, **P < 0.01 versus CTR or 0 h. (C) The secretion of cytokines was investigated using ELISA after dsDNA transfection for 24 h. Graph represents the concentration of cytokines in the supernatant normalized to the control and are shown as the means ± SEM of 6 independent experiments. *P < 0.05, **P < 0.01 vs. CTR.

2.2.7. Western blotting

Protein extracts were quantified using the bicinchoninic acid protein assay (Thermo scientific Pierce, USA). The prepared samples were subjected to 10–12% SDS-polyacrylamide gel electrophoresis and transferred onto 0.2 μm Immobilon® -P^{SQ} transfer membrane (Millipore, Germany). The primary antibodies were diluted 1:1000 for cGAS, STING, DNaseII, p-IRF3/IRF3, and p-p65/p65.

2.2.8. H&E staining and immunohistochemistry

For H&E staining, 7 μm synovial tissue sections from RA patients were deparaffinized and stained with haematoxylin and eosin (H&E). Histological scores of RA synovitis were graded using Krenn's synovitis score [12]. These scores included three basic morphological parameters: hyperplasia of the synovial lining layer, degree of inflammatory infiltration, and activation of synovial stroma. All parameters were graded as absent (0), slight [1], and moderate [2], to strong [3], and the sum scores of all parameters of the synovitis ranged from 0 to 9. RA patients were divided into slight synovitis (0–4) and strong synovitis groups [5–9] based on the sum scores. The samples were stained with anti-human cGAS antibody or isotype-matched antibody according to the manufacturer's instructions. Cells were visualized using a diaminobenzidine substrate. We used the immunoreactive score (IRS) proposed by Remmele and Stegner to evaluate the sections staining reactions [13]. IRS = PP (percentage of positive cells) × SI (staining intensity). The percentage of positive cells (PP) was graded as 0 (negative), 1 (10% positive cells), 2 (11–50% positive cells), 3 (51–80% positive cells), and 4 (> 80% positive cells). SI was scored as 0 (negative), 1 (weak), 2 (moderate), and 3 (strong). Ten different visual fields from each synovial section were observed for the IRS evaluation. Two separate observers performed all assessments in a blinded fashion.

2.3. Statistical analysis

All statistical analyses were performed using SPSS 13.0 statistical package. Data are expressed as the means ± SEM from at least 3 independent experiments. The data were analyzed in a blinded manner. When data of the mentioned variables were distributed normally, a 2-tailed Student's *t*-test was used to analyze the differences between two groups or one-way ANOVA analysis followed by Bonferroni's post hoc comparisons were performed for three or more groups. When data were not distributed normally, we used nonparametric tests (Mann–Whitney rank sum test for two groups or the Kruskal–Wallis one-way analysis among three groups for continuous variables) to compare the difference between different groups. Correlations analyses were analyzed using Spearman's rank order correlation test. *P* values less than or equal to 0.05 were considered significant.

3. Results

3.1. Accumulation of cytosolic dsDNA in FLS and synovial tissue from patients with rheumatoid arthritis

We determined the amount of cytosolic dsDNA in FLS from patients with trauma (healthy controls (HC)), RA and OA. Cytosolic dsDNA was measured using immunofluorescent staining. Compared to OA and HC FLS, dsDNA accumulation was more prominent in RA FLS (Fig. 1A). We further detected the dsDNA content in the cytoplasm of FLS using Qubit® dsDNA HS Assay Kits. The content of the cytosolic dsDNA was increased in RA FLS (Fig. 1B). TNF-α is a critical pro-inflammatory cytokine in RA. Therefore, we examined cytosolic dsDNA contents in RA FLS under TNF-α stimulation. RA FLS were stimulated with 10 ng/ml TNF-α for 12, 24 and 48 h. TNF-α treatment significantly increased cytosolic dsDNA in RA FLS at 24 h (Fig. 1C and D), whereas TNF-α had little effect on inducing dsDNA accumulation in OA FLS and HC FLS. (Fig. S1).

We measured cytosolic dsDNA expression in synovial tissue using immunofluorescent staining. Cytosolic dsDNA accumulated in RA synovial tissue, but this accumulation was less prominent in OA or HC tissues (Fig. 1E). We investigated cytosolic dsDNA expression in the synovium from different RA patients with different degrees of histological synovitis. The percentage of cytosolic dsDNA-positive cells was higher in RA patients with strong synovitis compared to RA patients with slight synovitis. Synovial cytosolic dsDNA intensity was also higher in RA patients with strong synovitis. We also found significant correlations between the cytosolic dsDNA immunoreactive score (IRS) and synovitis score ($r = 0.489$, $p = 0.013$) using Spearman's rank order correlation test (Fig. 1F). Collectively, our findings suggest that cytosolic dsDNA accumulation in FLS is associated with the severity of rheumatoid synovial inflammation.

3.2. Cytosolic dsDNA accumulation upregulated the production of pro-inflammatory cytokines and MMP in RA FLS

Cytosolic dsDNA triggers pro-inflammatory cytokines production in several other cell lines [14,15]. We evaluated the role of transfected cytosolic dsDNA in the production of pro-inflammatory cytokines and MMP. RA FLS were transfected with different sources of dsDNA (2 μg/ml), including HSV, *E. coli* and ISD dsDNA (45 bp dsDNA). The mRNA expression of IL-1β, TNF-α, MMP-13, CXCL-10, IL-6, IL-8, IFN-α and IFN-β increased after an 8 h transfection with these different sources of dsDNA. (Fig. 2A). We also examined the mRNA expression of these cytokines and MMP-13 in RA FLS transfected with 2 μg/ml of ISD dsDNA at different time points (4, 8 and 12 h) (Fig. 2B). We detected the secretion of these pro-inflammatory cytokines and MMP-13 after 2 μg/ml ISD dsDNA transfection into cytosol of RA FLS for 24 h and observed that these cytokines and MMP-13 increased after dsDNA transfection. These results suggest that the cytosolic dsDNA accumulation promotes the production of cytokines and MMP-13 in RA FLS (Fig. 2C). We also examined the mRNA expression and secretion of IFN-γ (type II IFNs), But IFN-γ have no evident changes (Fig. 2A, B and C).

3.3. DNaseII regulates the accumulation of cytosolic dsDNA and inflammatory cytokine and MMP secretion in RA FLS

DNaseII primarily digests cytosolic dsDNA in the cell cytosol. Therefore, we examined the interaction between DNaseII and cytosolic dsDNA in RA FLS. ISD dsDNA (2 μg/ml) was transfected into the cytosol of RA FLS, and the cytosolic dsDNA did not influence the DNaseII

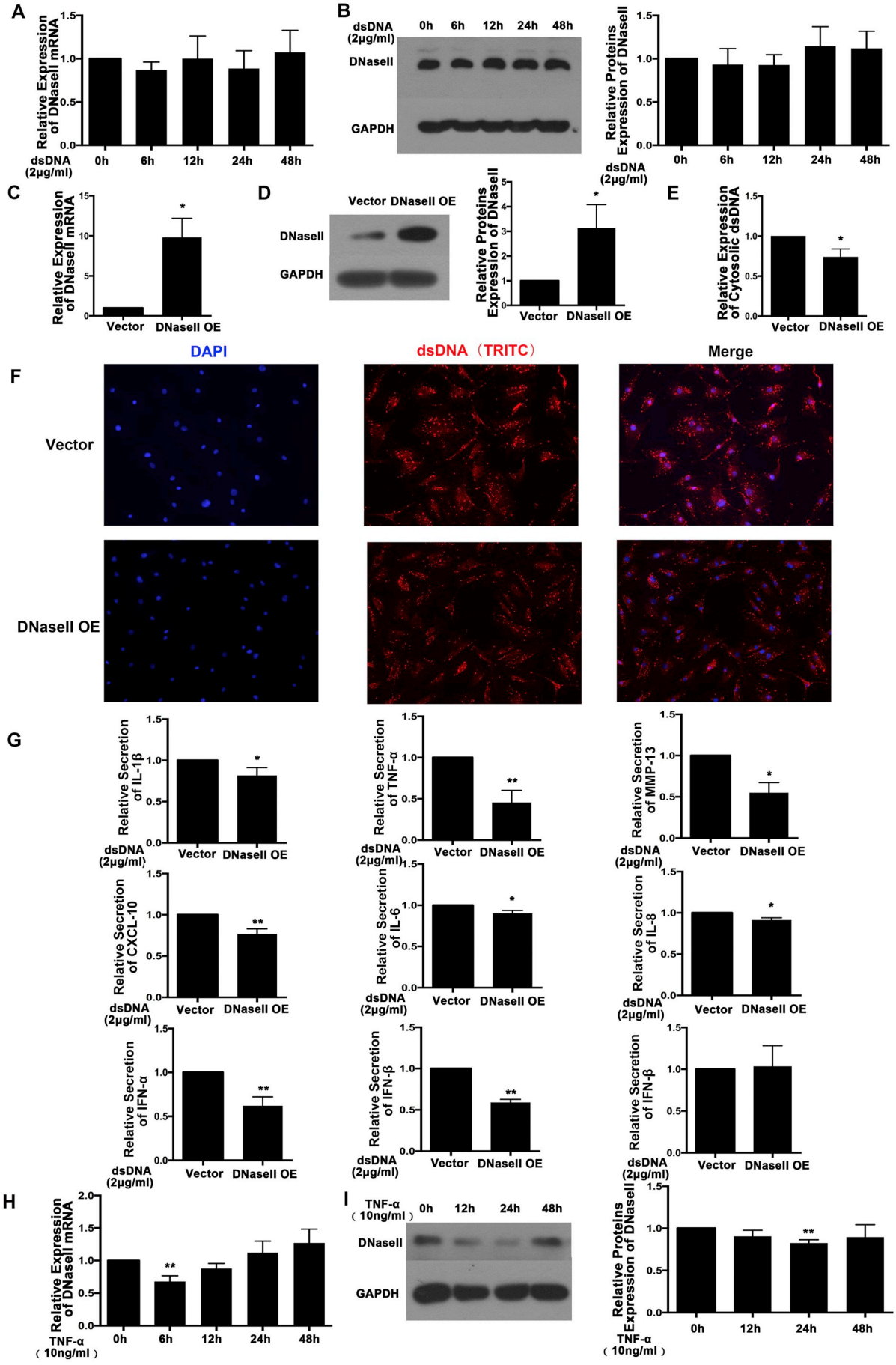

(caption on next page)

Fig. 3. *Effect of DNaseII on the RA FLS cytokine secretion.* (A) DNaseII mRNA expression was detected using real-time PCR. Graphs indicate the relative mRNA expression. (B) Protein expression of DNaseII was measured using Western blotting. Representative images of immune blots (left panel) and densitometric quantification (right panel) of DNaseII expression from 6 independent experiments. Values were normalized to the 0 h group. (C and D) The gene (C) and protein expression (D) of DNaseII were detected using real-time PCR and Western blotting after lentiviral-mediated gene transfection, respectively. Values were normalized to the vector group. *P < 0.05 versus vector, using Student's *t*-test. (E and F) The dsDNA content in the cytosol of RA FLS was measured using the Qubit® dsDNA HS Assay (E) and immunofluorescent staining (F). RA FLS were infected with control lentivirus (as Vector) or DNaseII and serum-starved overnight and transfected with dsDNA (2 μg/ml) for 12 h. Values were normalized to the vector group. *P < 0.05 versus vector, using Student's t-test. (G) IL-1β, TNF-α, MMP-13, CXCL-10, IL-6, IL-8, IFN-α, IFN-β and IFN- γ secretion was determined using ELISA. Values were normalized to the vector group. *$P < 0.05$, **$P < 0.01$ versus vector, using Student's *t*-test. (H and I) TNF-α (10 ng/ml) was added to the RA FLS, and the gene and protein expression of DNaseII were detected using real-time PCR and Western blotting, respectively. Values were normalized to the 0 h group. *$P < 0.05$, **$P < 0.01$ versus 0 h, using one-way ANOVA assay with Bonferroni's post hoc comparison.

mRNA or protein expression (Fig. 3A and B). We further evaluated the effect of DNaseII overexpression on cytosolic dsDNA accumulation using immunofluorescence staining and Qubit® dsDNA HS Assay Kits. RA FLS were overexpressed with DNaseII using lentiviral-mediated gene transfection and transfected with dsDNA. Transfection with lentiviral-mediated DNaseII overexpression efficiently and specifically enhanced DNaseII expression (Fig. 3C and D). DNaseII overexpression reduced the cytosolic dsDNA contents compared to the control vector (Fig. 3E and F). Transfection with overexpressed DNaseII inhibited the dsDNA-induced secretion of IL-1β, TNF-α, MMP-13, CXCL-10, IL-6, IL-8, IFN-α and IFN-β in RA FLS, but not IFN-γ (Fig. 3G).

DNaseII expression was decreased in RA FLS compared to HC FLS (data not shown). TNF-α stimulation for 6 h and 24 h reduced DNaseII mRNA and protein expression, respectively (Fig. 3H and I). Collectively, our data suggest that increased cytosolic dsDNA is associated with the reduction of DNaseII expression in RA FLS.

3.4. The cGAS/STING pathway mediates the cytosolic dsDNA-induced inflammatory response in RA FLS

Previous studies demonstrated that cGAS was a specific receptor for cytosolic dsDNA [2]. Therefore, we examined whether cGAS was involved in cytosolic dsDNA-induced inflammatory response in RA FLS. We measured the expression pattern of cGAS in FLS and synovium and found increased cGAS expression in RA FLS compared to OA FLS and HC FLS using immunofluorescence staining (Fig. 4A), which was confirmed using Western blotting (Fig. 4B). We also determined that cGAS expression was increased in synovial tissue from RA patients compared to OA patients and HC (Fig. 4C). We observed a positive correlation between the cGAS immunoreactive score (IRS) and synovitis score ($r = 0.558$, $p = 0.04$) using Spearman's rank order correlation test (Fig. 4D). These data indicate that increased cGAS expression was associated with rheumatoid arthritis synovial inflammation.

We clarified whether the accumulation of cytosolic dsDNA induced the expression of cGAS and its downstream signal protein STING. cGAS and STING mRNA expression increased after various dsDNA transfection for 8 h, including HSV, *E. coli* and ISD dsDNA (Fig. 4E). We found that the mRNA and protein expression of cGAS and STING varied at different time points following ISD dsDNA transfection (Fig. 4F and G). We determined that TNF-α stimulation increased mRNA and protein expression of cGAS and STING (Fig. 4H and I).

Finally, we investigated whether cGAS/STING pathway was involved in cytosolic dsDNA-induced inflammation in RA FLS. We used the RNA interference technique to knockdown cGAS and STING expression. cGAS shRNA and STING shRNA reduced the mRNA and protein expression of cGAS and STING, respectively (Fig. 4J). We demonstrated that treatment with cGAS shRNA or STING shRNA reduced dsDNA-induced secretion of IL-1β, TNF-α, MMP-13, CXCL-10, IL-6, IL-8, IFN-α and IFN-β compared to the control shRNA treatment, but not IFN-γ (Fig. 4K). In the presence of TNF-α, cytokine signaling are activated which are suppressed by knockdown of cGAS and STING (Fig. 4L). Taken together, our data suggest that the cGAS/STING pathway is involved in cytosolic dsDNA-induced synovial inflammation in RA.

3.5. DNaseII overexpression and cGAS/STING knockdown prevents NF-κB and IRF3 activation in RA FLS

Increased expression of cGAS/STING activates NF-κB and transcription factor IFR3 pathway in several cell lines [16]. Therefore, we performed the NF-κB subunit p65 nuclear translocation assay using immunofluorescence to investigate the effect of dsDNA on the NF-κB pathway. Transfection with dsDNA (2 μg/ml) for 1 h promoted the translocation of p65 into the nucleus from the cytoplasm, but transfection with overexpressed DNaseII or shRNA for cGAS or STING reduced this translocation (Fig. 5A and B). Western blotting also demonstrated that transfection with overexpressed DNaseII or knockdown of cGAS or STING suppressed transfected dsDNA-induced phosphorylation of p65 (Fig. 5C). We evaluated the role of DNaseII and cGAS/STING in the regulation of IRF3 activation. dsDNA transfection increased IRF3 phosphorylation (Fig. 5D), and DNaseII overexpression or knockdown of cGAS or STING inhibited this increase (Fig. 5E).

We elucidated the relationship of DNaseII and cGAS/STING. DNaseII overexpression reduced the expression of cGAS and STING, but cGAS or STING knockdown did not influence DNaseII expression (Fig. 5F and G). cGAS knockdown decreased the dsDNA-induced STING expression, but STING knockdown did not affect dsDNA-induced cGAS expression. Collectively, these findings suggest that DNaseII and cGAS/STING are involved in cytosolic dsDNA-induced activation of NF-κB and IRF3.

4. Discussion

The present study observed elevated cytosolic dsDNA accumulation and cGAS/STING expression and decreased DNaseII expression in RA FLS. Increased dsDNA accumulation and cGAS expression in synovial tissue positively correlated with the severity of RA synovitis. TNF-α treatment increased cytosolic dsDNA accumulation and cGAS/STING expression and decreased DNaseII expression in RA FLS. Transfection with exogenous dsDNA into the cytoplasm of RA FLS induced the production of pro-inflammatory cytokines, MMP-13, and cGAS/STING in RA FLS. DNaseII overexpression and cGAS/STING knockdown decreased the cytosolic dsDNA-induced cytokine production. Collectively, our data demonstrate that cytosolic dsDNA accumulation is associated with decreased DNaseII expression and contributes to the inflammatory responses via regulation of the cGAS/STING pathway in RA FLSs (Fig. 6). These findings support the contribution of cytosolic dsDNA in RA FLS to synovial inflammation in RA.

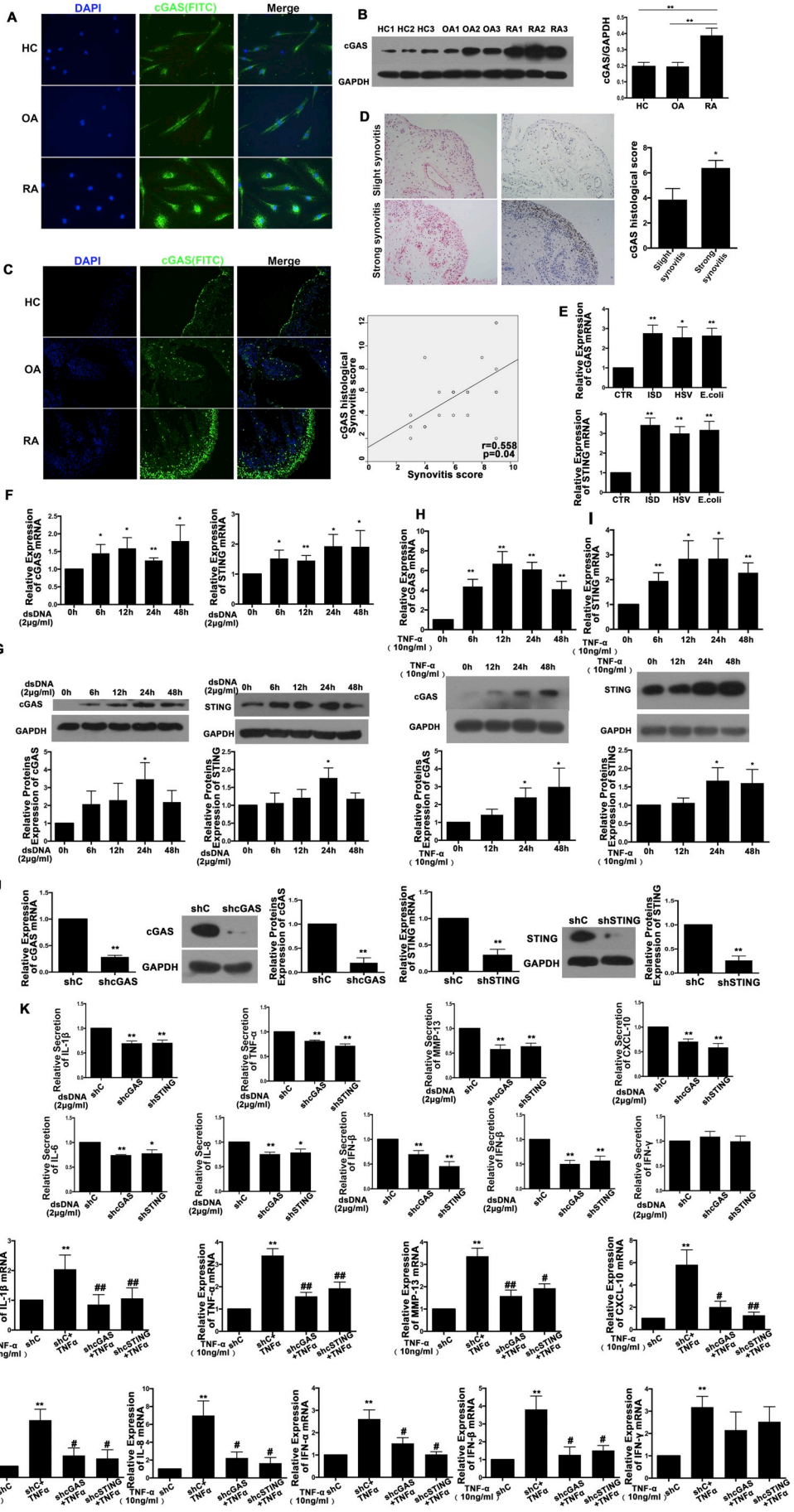

(caption on next page)

Fig. 4. *Cytosolic dsDNA and TNF-α activated the cGAS/STING pathway.* (A and B) cGAS expression in FLS was detected using immunofluorescent staining and Western blotting. Representative immunofluorescent images of dsDNA (green) and nuclei (blue) in FLS from HC ($n = 4$) and patients with OA ($n = 6$) and RA ($n = 8$). Representative images of immunoblots (left panel), and densitometric quantification (right panel) of cGAS expression in FLS from HC (n = 6) and patients with OA (n = 6) and RA (n = 6). The values are presented as the means ± SEM of 6 independent experiments. $^{**}P < 0.01$ vs. HC or OA, using one-way ANOVA assay with Bonferroni's post hoc comparison. (C) cGAS expression in the synovium from HC (n = 4), OA patients (n = 6) and RA patients (n = 8). (original magnification 200 ×) (D) cGAS expression and synovitis evaluation were detected using immunohistochemistry and H&E staining, respectively. Graph indicates cGAS histological scores in slight and strong synovitis. Data are shown as the means ± SEM of 24 independent experiments of 24 different RA patients. $^{*}P < 0.05$, versus slight synovitis, using Student's *t*-test. Correlations were analyzed using Spearman's rank order correlation test. (E) RA FLS were transfected with HSV, *E. coli*, and ISD dsDNA (2 μg/ml) for 8 h. The cGAS and STING mRNA expression were measured using real-time PCR. (F and G) RA FLS were transfected with ISD dsDNA (2 μg/ml) for different times (6, 12, 24 and 48 h). The cGAS and STING gene and protein expression were measured using real-time PCR and Western blots, respectively. Representative images of immunoblots (upper panel) and densitometric quantification (lower panel) of cGAS and STING expression in the FLS are shown. (H and I) RA FLS were treated with TNF-α (10 ng/ml) for 6 h, 12 h, 24 h and 48 h. The cGAS and STING gene and protein expression were detected using real-time PCR and Western blotting, respectively. Representative images of immunoblots (upper panel) and densitometric quantification (lower panel) of cGAS and STING expression in the FLS are shown. (J) RA FLS were infected with control lentivirus (as shC) or shcGAS or shSTING for knockdown of cGAS and STING. The cGAS and STING gene and protein expression were investigated using real-time PCR and Western blot, respectively. Values were normalized to shC group. $^{*}P < 0.05$, $^{**}P < 0.01$ versus the shC group, using Student's *t*-test. (K) Inflammatory cytokine (IL-1β, TNF-α, CXCL-10, IL-6, IL-8, IFN-α, IFN-β and IFN-γ) secretion and MMP13 were measured using ELISA. (E, E, G, H, I and K) Values were normalized to CTR or shC or 0 h groups. $^{*}P < 0.05$, $^{**}P < 0.01$ versus CTR or shC or 0 h, using one-way ANOVA assay with Bonferroni's post hoc comparison. (L) RA FLS were treated with TNF-α (10 ng/ml) for 24 h. Cytokines (IL-1β, TNF-α, MMP-13, CXCL-10, IL-6, IL-8, IFN-α, IFN-β and IFN-γ) mRNA expression was measured using real-time PCR. The values are presented as the means ± SEM of 6 independent experiments. Values were normalized to the shC group. $^{*}P < 0.05$, $^{**}P < 0.01$ versus shC, $^{\#}P < 0.05$, $^{\#\#}P < 0.01$ versus shC + TNF-α, using Student's t-test or one-way ANOVA assay with Bonferroni's post hoc comparison. shC, control lentivirus; HC, healthy control; 0 h, 0 h; CTR, control. (For interpretation of the references to colour in this figure legend, the reader is referred to the web version of this article.)

Cytosolic dsDNA sensing triggers innate immune responses, which provide protection against viral or bacterial infection, contribute to autoimmune disease and generate anti-tumor adaptive immunity [17]. DNA fragments are detected in the cytosol of epidermal keratinocytes from psoriatic lesions, and these fragments contribute to inflammation via activation of IL-1β [9]. MUS81-induced cytosolic dsDNA in prostate cancer cells from hyperplasia to clinical stage II prostate cancers causes cancer-specific T cell responses [18]. The presence of dsDNA in the cytosol of B cell lymphoma from transgenic Eμ-*Myc* C57BL/6 mice exerts tumor immunosurveillance activity via activation of the STING-DNA sensor pathway [19]. These studies suggest that the enrichment of dsDNA in the cytosol facilitates inflammatory disease and tumor surveillance. However, little is known about the effect of cytosolic dsDNA on the pathogenesis of RA. Our results indicate that dsDNA was prominent in the synovium and cytosol of FLS from RA patients. Cytosolic dsDNA promoted inflammatory cytokine secretion of RA FLS. These results demonstrate that cytosolic dsDNA evokes inflammatory responses in RA FLS.

DNA is located in the mitochondria and nucleus, rather than the cytosol, under normal physiological conditions. Cytosolic dsDNA accumulation occurs when extracellular dsDNA is transported into the cytosol or endogenous dsDNA homeostatic elimination is hampered. Microbial infection delivers microbial DNA to the cell cytoplasm, but self-DNA also enters into the cytosol [20]. Extracellular self-dsDNA enters into the cytosol of monocytes via peptide LL-37 and leads to type I IFN induction and inflammatory responses [21]. Previous studies revealed a substantial increase in cfDNA concentrations in sera and synovial fluid from RA patients [22–24]. The levels of cfDNA in sera from RA patients were related with the severity of joint symptoms [24]. We also found that dsDNA stimulation without transfection reagent increased cytokine gene expression in RA FLS (unpublished data). This result indicates that increased cytosolic dsDNA accumulation in RA FLS may be partially due to increased levels of dsDNA in the synovial extracellular microenvironment. However, cytosolic dsDNA accumulation is associated with a deficiency of endogenous DNA elimination. Nucleases in the cell degrade endogenous DNA under physiological conditions. There are two critical nucleases, DNaseII and TREX1, that prevent DNA accumulation in the cytosol. Trex1 degrades single-stranded DNA, and DNaseII targets dsDNA. However, cytosolic DNA accumulates in the cytosol when DNaseII activity is inefficient or impaired, which results in serious and detrimental problems. DNaseII$^{-/-}$IFN-IR$^{-/-}$ mice develop chronic polyarthritis and exhibit an upregulation of cytokines, MMPs and autoimmune autoantibodies, such as anti-CCP and RF, in sera which is similar to human rheumatoid arthritis [25,26]. Further study found that macrophages from DNaseII$^{-/-}$IFN-IR$^{-/-}$ mice cannot degrade dsDNA and contained higher levels of dsDNA in the cytosol. These macrophages produced TNF-α and other cytokines and contributed to the activation of fibroblast-like synoviocytes [27,28]. Our results demonstrated that the TNF-α stimulation downregulated DNaseII expression and upregulated dsDNA content in the cytosol. We also found that DNaseII overexpression reduced the dsDNA-induced content of cytosolic dsDNA in RA FLS, inhibited cGAS and STING expression and pro-inflammatory cytokine secretion. These findings suggest that increased cytosol dsDNA accumulation in RA FLS is related to the transport of dsDNA in the extracellular environment, and the abnormal accumulation of dsDNA in the cytosol resulting from the inadequate capabilities of DNaseII.

cGAS, IFI16, DDX41, DAI, and DNA-PK sense cytosolic DNA. cGAS is an essential cytosolic DNA sensor [1,29,30]. cGAS conformation changes after dsDNA binding and provides access to cytosolic ATP and GTP, which are used to synthesis cGAMP. cGAMP is a second messenger that activates the adaptor protein STING, which recruits the downstream IFR3 for IFN production and NF-κB for cytokine release. The dsDNA-cGAS/STING pathway leads to a protective immune defense and autoimmunity and inflammatory disease. cGAS and STING deletion in DNaseII$^{-/-}$ IFN-IR$^{-/-}$ mice relieved the polyarthritis symptoms of mice [31,32]. Fibroblasts, macrophages, and dendritic cells from cGAS-deficient (cGAS$^{-/-}$) mice secrete little type I IFN and pro-inflammatory cytokines after DNA transfection into cells [20,29]. These findings implicate cGAS/STING pathway as the key regulator in dsDNA-induced inflammatory responses. Our results also demonstrated that cGAS and STING knockdown inhibited dsDNA-induced pro-inflammatory cytokine secretion. We further demonstrated that overexpression of DNaseII and deletion of cGAS or STING inhibited the dsDNA-induced activation of IRF3 and NF-κB. However, little is known about the effect of DNaseII overexpression on cGAS and STING expression. We found that DNaseII overexpression induced decreased gene and protein expression of cGAS and STING. These results demonstrated that cytosolic dsDNA was

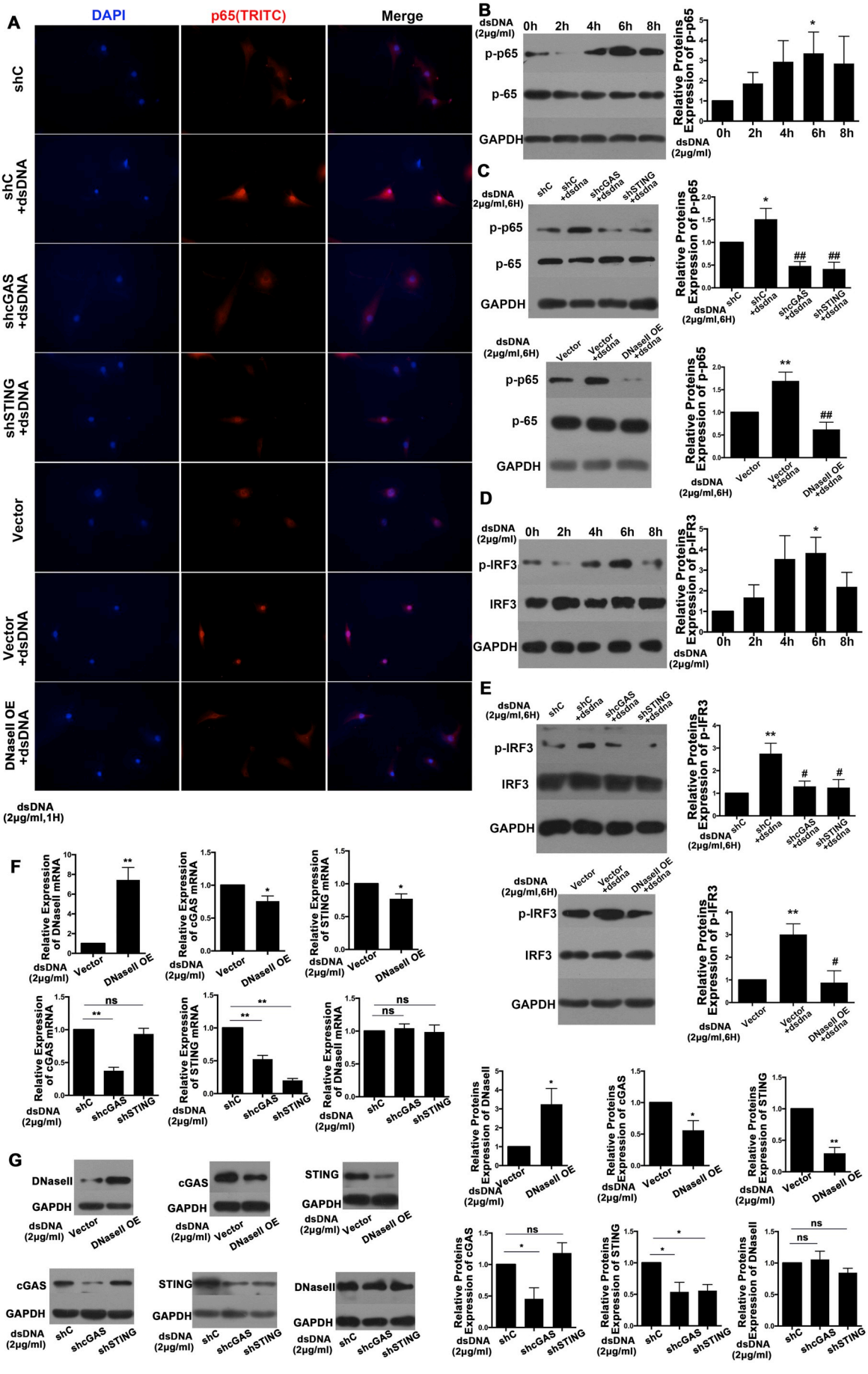

(caption on next page)

Fig. 5. Effect of DNaseII overexpression and cGAS /STING knockdown on the IRF3 and NF-κB activation. (A) The entrance of p65 into the nucleus was evaluated using immunofluorescence. Representative immunofluorescent images of p65 (red) and nuclei (blue) in FLS are shown. Original magnification 200×. (B, C, D and E) With or without infection of control lentivirus (as shC and Vector) or shcGAS or shSTING or DNaseII OE, RA FLS were serum-starved overnight and transfected with dsDNA (2 μg/ml) for different time. The phosphorylation of p65(Ser536) and IRF3(Ser396) was evaluated using Western blotting. Representative images of immunoblots (left panel) and densitometric quantification (right panel) of p-p65 and p-IRF3 expression are shown. Values were normalized to 0 h or shC or vector. *P < 0.05, **P < 0.01 versus 0 h or shC or vector, #P < 0.05, ##P < 0.01 versus shC (or vector) + dsDNA, using one-way ANOVA assay with Bonferroni's post hoc comparison. (F and G) The gene and protein expression of DNaseII, cGAS and STING were measured using real-time PCR and Western blotting, respectively. Representative images of immunoblots (left panel) and densitometric quantification (right panel) of DNaseII, cGAS and STING expression are shown. Values were normalized to shC or vector. *P < 0.05, **P < 0.01 versus shC or vector, using Student's *t*-test or one-way ANOVA assay with Bonferroni's post hoc comparison. ns, no significance. (For interpretation of the references to colour in this figure legend, the reader is referred to the web version of this article.)

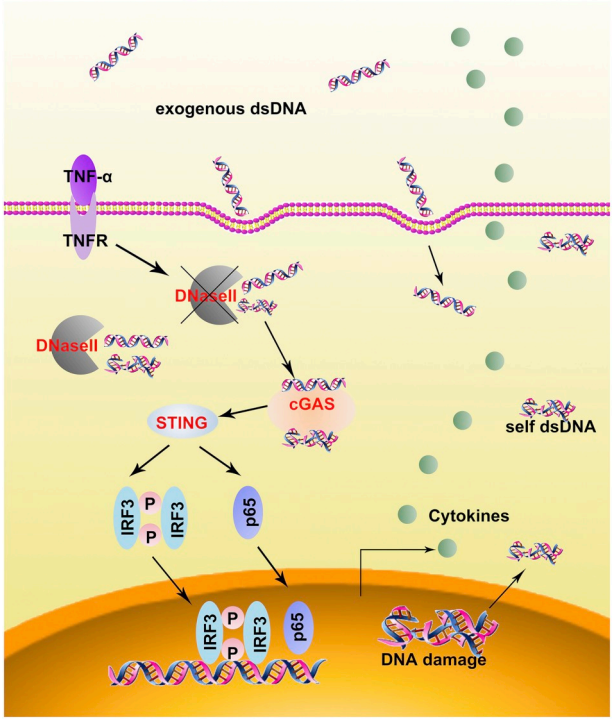

Fig. 6. Proposed model for the role of increased cytosolic dsDNA in the regulation of synovial inflammation in patients with rheumatoid arthritis.

involved in the cytokine production of RA FLS via the DNaseII-cGAS-STING-IRF3/NF-κB pathway.

In summary, our findings demonstrated that aberrant dsDNA accumulation in the cytosol of RA FLS exerted an important role in the promotion of rheumatoid synovial inflammation via regulation of the cGAS/STING pathway. These findings provide a novel insight in the pathogenesis of RA.

Supplementary data to this article can be found online at https://doi.org/10.1016/j.intimp.2019.105791.

Declaration of competing interest

The authors have no financial conflicts of interest.

References

[1] R.E. Vance, Cytosolic DNA sensing: the field narrows, Immunity 45 (2016) 227–228.
[2] X. Li, C. Shu, G. Yi, C.T. Chaton, C.L. Shelton, J. Diao, X. Zuo, C.C. Kao, A.B. Herr, P. Li, Cyclic GMP-AMP synthase is activated by double-stranded DNA-induced oligomerization, Immunity 39 (2013) 1019–1031.
[3] N. Bottini, G.S. Firestein, Duality of fibroblast-like synoviocytes in RA: passive responders and imprinted aggressors, Nat. Rev. Rheumatol. 9 (2013) 24–33.
[4] I.B. McInnes, G. Schett, The pathogenesis of rheumatoid arthritis, New Engl. J. Med. 365 (2011) 2205–2219.
[5] Y. Wang, G.H. Su, F. Zhang, J.X. Chu, Y.S. Wang, Cyclic GMP-AMP synthase is required for cell proliferation and inflammatory responses in rheumatoid arthritis synoviocytes, Mediat. Inflamm. 2015 (2015) 192329.
[6] X. Cai, Y.H. Chiu, Z.J. Chen, The cGAS-cGAMP-STING pathway of cytosolic DNA sensing and signaling, Mol. Cell 54 (2014) 289–296.
[7] K. Kis-Toth, A. Szanto, T.H. Thai, G.C. Tsokos, Cytosolic DNA-activated human dendritic cells are potent activators of the adaptive immune response, J. Immunol. 187 (2011) 1222–1234.
[8] L. Ponomareva, H. Liu, X. Duan, E. Dickerson, H. Shen, R. Panchanathan, D. Choubey, AIM2, an IFN-inducible cytosolic DNA sensor, in the development of benign prostate hyperplasia and prostate cancer, Mol. Cancer Res. 11 (2013) 1193–1202.
[9] J. Schauber, Y. Dombrowski, R. Besch, Pathogenic DNA: cytosolic DNA promotes inflammation in psoriasis, Cell Cycle 10 (2011) 3038–3039.
[10] D. Aletaha, T. Neogi, A.J. Silman, J. Funovits, D.T. Felson, C.O. Bingham, N.S. Birnbaum 3rd, G.R. Burmester, V.P. Bykerk, M.D. Cohen, B. Combe, K.H. Costenbader, M. Dougados, P. Emery, G. Ferraccioli, J.M. Hazes, K. Hobbs, T.W. Huizinga, A. Kavanaugh, J. Kay, T.K. Kvien, T. Laing, P. Mease, H.A. Menard, L.W. Moreland, R.L. Naden, T. Pincus, J.S. Smolen, E. Stanislawska-Biernat, D. Symmons, P.P. Tak, K.S. Upchurch, J. Vencovsky, F. Wolfe, G. Hawker, 2010 rheumatoid arthritis classification criteria: an American College of Rheumatology/European league against rheumatism collaborative initiative, Arthritis Rheum. 62 (2010) 2569–2581.
[11] H. Wang, J. Wu, X. Liu, H. He, F. Ding, H. Yang, L. Cheng, W. Liu, J. Zhong, Y. Dai, G. Li, C. He, L. Yu, J. Li, Identification of short hairpin RNA targeting foot-and-mouth disease virus with transgenic bovine fetal epithelium cells, PLoS One 7 (2012) e42356.
[12] V. Krenn, L. Morawietz, T. Haupl, J. Neidel, I. Petersen, A. Konig, Grading of chronic synovitis–a histopathological grading system for molecular and diagnostic pathology, Pathol. Res. Pract. 198 (2002) 317–325.
[13] W. Remmele, H.E. Stegner, Recommendation for uniform definition of an immunoreactive score (IRS) for immunohistochemical estrogen receptor detection (ER-ICA) in breast cancer tissue, Pathologe 8 (1987) 138–140.
[14] J. Ahn, D. Gutman, S. Saijo, G.N. Barber, STING manifests self DNA-dependent inflammatory disease, Proc. Natl. Acad. Sci. U. S. A. 109 (2012) 19386–19391.
[15] V. Hornung, E. Latz, Intracellular DNA recognition, Nat Rev Immunol 10 (2010) 123–130.
[16] R. Fang, C. Wang, Q. Jiang, M. Lv, P. Gao, X. Yu, P. Mu, R. Zhang, S. Bi, J.M. Feng, Z. Jiang, NEMO-IKKbeta are essential for IRF3 and NF-kappaB activation in the cGAS-STING pathway, J. Immunol. 199 (2017) 3222–3233.
[17] G.N. Barber, STING: infection, inflammation and cancer, Nat Rev Immunol 15 (2015) 760–770.
[18] S.S. Ho, W.Y. Zhang, N.Y. Tan, M. Khatoo, M.A. Suter, S. Tripathi, F.S. Cheung, W.K. Lim, P.H. Tan, J. Ngeow, S. Gasser, The DNA structure-specific endonuclease MUS81 mediates DNA sensor STING-dependent host rejection of prostate cancer cells, Immunity 44 (2016) 1177–1189.
[19] A.R. Lam, N.L. Bert, S.S. Ho, Y.J. Shen, L.F. Tang, G.M. Xiong, J.L. Croxford, C.X. Koo, K.J. Ishii, S. Akira, D.H. Raulet, S. Gasser, RAE1 ligands for the NKG2D receptor are regulated by STING-dependent DNA sensor pathways in lymphoma, Cancer Res. 74 (2014) 2193–2203.
[20] Q. Chen, L. Sun, Z.J. Chen, Regulation and function of the cGAS-STING pathway of cytosolic DNA sensing, Nat. Immunol. 17 (2016) 1142–1149.
[21] G. Chamilos, J. Gregorio, S. Meller, R. Lande, D.P. Kontoyiannis, R.L. Modlin, M. Gilliet, Cytosolic sensing of extracellular self-DNA transported into monocytes by the antimicrobial peptide LL37, Blood 120 (2012) 3699–3707.
[22] E. Bartoloni, V. Ludovini, A. Alunno, L. Pistola, O. Bistoni, L. Crino, R. Gerli, Increased levels of circulating DNA in patients with systemic autoimmune diseases: a possible marker of disease activity in Sjogren's syndrome, Lupus 20 (2011) 928–935.
[23] X.Y. Zhong, I. von Muhlenen, Y. Li, A. Kang, A.K. Gupta, A. Tyndall, W. Holzgreve, S. Hahn, P. Hasler, Increased concentrations of antibody-bound circulatory cell-free DNA in rheumatoid arthritis, Clin. Chem. 53 (2007) 1609–1614.
[24] S.A. Leon, G.E. Ehrlich, B. Shapiro, V.A. Labbate, Free DNA in the serum of rheumatoid arthritis patients, J. Rheumatol. 4 (1977) 139–143.
[25] K. Kawane, M. Ohtani, K. Miwa, T. Kizawa, Y. Kanbara, Y. Yoshioka, H. Yoshikawa, S. Nagata, Chronic polyarthritis caused by mammalian DNA that escapes from degradation in macrophages, Nature 443 (2006) 998–1002.
[26] H. Yoshida, Y. Okabe, K. Kawane, H. Fukuyama, S. Nagata, Lethal anemia caused by interferon-beta produced in mouse embryos carrying undigested DNA, Nat. Immunol. 6 (2005) 49–56.
[27] R. Baum, S. Sharma, J.M. Organ, C. Jakobs, V. Hornung, D.B. Burr, A. Marshak-Rothstein, K.A. Fitzgerald, E.M. Gravallese, STING contributes to abnormal bone formation induced by deficiency of DNase II in mice, Arthritis Rheumatol 69 (2017) 460–471.
[28] K. Kawane, H. Tanaka, Y. Kitahara, S. Shimaoka, S. Nagata, Cytokine-dependent but

acquired immunity-independent arthritis caused by DNA escaped from degradation, Proc. Natl. Acad. Sci. U. S. A. 107 (2010) 19432–19437.
[29] X.D. Li, J. Wu, D. Gao, H. Wang, L. Sun, Z.J. Chen, Pivotal roles of cGAS-cGAMP signaling in antiviral defense and immune adjuvant effects, Science 341 (2013) 1390–1394.
[30] J.W. Schoggins, D.A. MacDuff, N. Imanaka, M.D. Gainey, B. Shrestha, J.L. Eitson, K.B. Mar, R.B. Richardson, A.V. Ratushny, V. Litvak, R. Dabelic, B. Manicassamy, J.D. Aitchison, A. Aderem, R.M. Elliott, A. Garcia-Sastre, V. Racaniello, E.J. Snijder, W.M. Yokoyama, M.S. Diamond, H.W. Virgin, C.M. Rice, Pan-viral specificity of IFN-induced genes reveals new roles for cGAS in innate immunity, Nature 505 (2014) 691–695.
[31] D. Gao, T. Li, X.D. Li, X. Chen, Q.Z. Li, M. Wight-Carter, Z.J. Chen, Activation of cyclic GMP-AMP synthase by self-DNA causes autoimmune diseases, Proc. Natl. Acad. Sci. U. S. A. 112 (2015) E5699–E5705.
[32] K. Motani, S. Ito, S. Nagata, DNA-mediated cyclic GMP-AMP synthase-dependent and -independent regulation of innate immune responses, J. Immunol. 194 (2015) 4914–4923.